ISTITUTO NAZIONALE DI FISICA NUCLEARE

Sezione di Bari

INFN/BE-83/9
2 Novembre 1983

R. De Leo, G. D'Erasmo, S. Micheletti, A. Pantaleo,
V. Paticchio, M. Pignanelli and V. Variale:

CARBON FRAGMENTATION DATA FROM 37 AND 40 MeV PROTON BOMBARDMENT

Istituto Nazionale di Fisica Nucleare
Sezione di Bari

INFN/BE-83/9
2 Novembre 1983

CARBON FRAGMENTATION DATA FROM 37 AND 40 MeV PROTON BOMBARDMENT

R. De Leo, G. D'Erasmo, A. Pantaleo, V. Paticchio, V. Variale
INFN - Sezione di Bari, and Dipartimento di Fisica dell'Università di Bari

S. Micheletti, M. Pignanelli
INFN - Sezione di Milano, and Dipartimento di Fisica dell'Università di Milano

1. - INTRODUCTION

The aim of this work is to report on the experimental results obtained in the study of fragmentation reactions induced by 37 and 40 MeV protons on Carbon. The investigation at 37 MeV incident energy was first undertaken with the aim of obtaining cross sections for the production of masses from A = 6 to A = 11 which are relevant to the astrophysical problem of Li-Be-B densities in the universe[1, 2].

In the analysis of these data it was clearly seen that a big fraction of the production cross section for masses A = 6 and A = 7 was accounted for by monokinetic peaks at the high energy edge of the spectra. The energies of these peaks were consistent with the identification of the direct reaction $^{12}C(p, ^{6}Li)^{7}Be$.

To resolve the 0.431 MeV first excited level of ^{7}Be, a second measurement was carried out with improved energy resolution and increased number of angles at 40.3 MeV proton incident energy, in which the attention was focused onto the direct transfer reaction $^{12}C(p, ^{6}Li)^{7}Be_{g.s.}$ and $^{12}C(p, ^{6}Li)^{7}Be_{0.431\,MeV}$. The cross section obtained in these measurements are reported in the following with graphs and tables. Some detail of the experimental method is given in section 2, together with comments on data reduction. No attempt is made here to analyze the results in the framework of nuclear models and reaction mechanisms or to compare our data with the literature, being these studies in progress up to now.

2. - EXPERIMENTAL METHOD AND DATA REDUCTION

The energy analyzed proton beam of the Milan AVF cyclotron was focused onto 30 to 100 $\mu g/cm^2$ self supporting carbon targets.

In the 37 MeV measurements the target was put in a "small" scattering chamber with 70 cm diameter, while in the 40.3 MeV measurement the scattering chamber used was 120 cm diameter, thus allowing longer flight bases and best resolutions in the time of flight (TOF) measurements. The detectors were aimed to detect energy and TOF of the fragments. The energy was measured by means of a 300 μm thick surface barrier totally depleted silicon detector. For the TOF two trasmission time detectors were provided in which the electrons stripped by the fragments passing through thin carbon foils are accelerated and bent onto Micro-Channel Plate (MCP) electron multipliers. More details concerning these time detectors (Fig. 1) and their detection efficiencies to light ions can be found elsewhere[3]. The choice of both start and stop MCP detectors was made on account of the better timing resolution obtained, typically less than 200 psec during four hours continuous data taking. In the 37 MeV measurements the maximum allowed flight base was 17 cm which allowed a mass resolution better than 3.9%, while in the 40.3 MeV run the flight base used was 25 cm long, giving a $\Delta m/m$ of about 3%. In the latter measurement the maximum care was taken to minimize the energy spreads due to beam transport and fragment straggling in the target and strippers, achieving a reasonable compromise with counting rate and statistics at 220 keV FWHM energy resolution. In Fig. 2 sketches can be seen of the experimental apparatus and electronics set-up used.

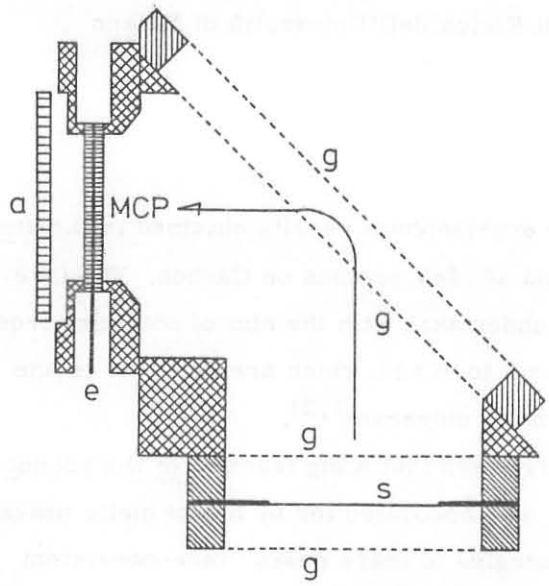

FIG. 1 - Trasmission time detector view. S = carbon foil electron stripper; g = harpes to apply accelerating and bending potentials for the stripped electrons; MCP= = Micro-Channel plates in Chevron configuration; e = a thin electrode between the two MCPs; a = anode.

Energy and TOF spectra were fed event by event into the on-line PDP 11/34 computer and the following analysis identified clearly the different mass ejectiles. Fig. 3 shows a cut in the E*TOF matrix at $E = 4.9 \pm 0.1$ MeV with an indication of the ejectile masses clearly identified. Fig. 4 shows energy spectra for masses A = 6 and A = 7

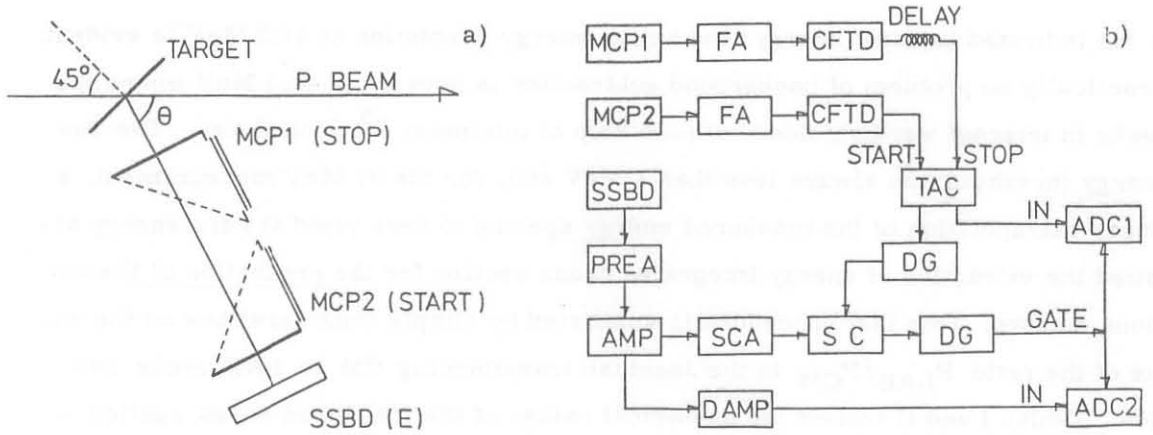

FIG. 2 - a) Experimental lay-out. MCP1 and MCP2 are the two trasmission time detectors. SSBD is a surface barrier totally depleted silicon detector. b) A block diagram of the electronics. FA = fast amplifier; CFTD = constant fraction timing discriminator; TAC = time to amplitude converter; DG = delay generator; PREA = preamplifier; AMP = amplifier; SCA = single channel analyzer; SC = slow coincidence; DAMP = delay amplifier; ADC1/2 = analog to digital converter.

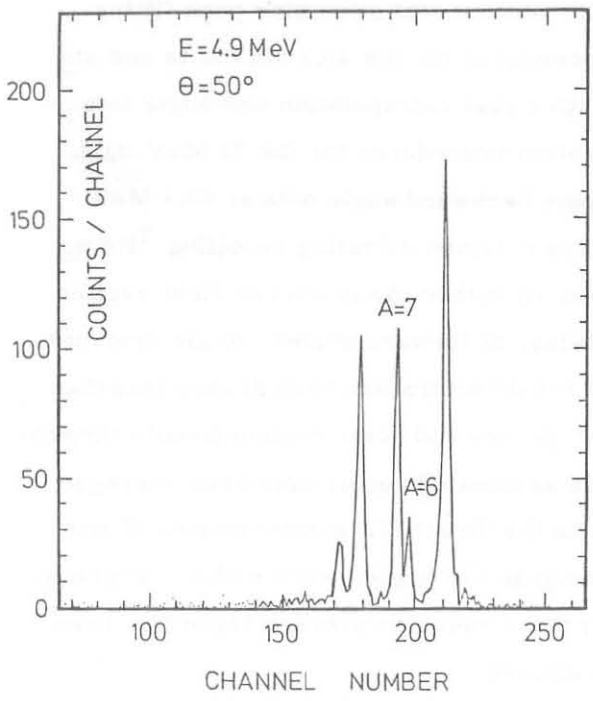

FIG. 3 - Time of flight of different mass ejectiles at 4.9 ± 0.1 MeV (zero time to the right). The energy bin has been enlarged for sake of statistics.

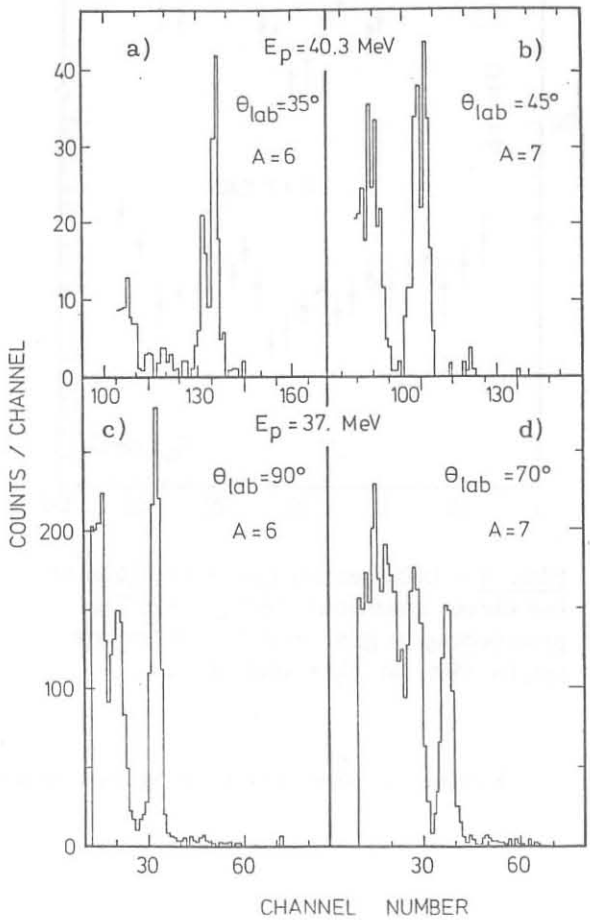

FIG. 4 - Typical energy spectra for the masses A = 6 and A = 7 at 40.3 MeV, a) and b), and at 37 MeV, c) and d).

at the indicated incident energy: the better energy resolution at 40.3 MeV is evident. Practically no problem of background subtraction is present at 40.3 MeV where the peaks in interest were unfolded with the help of minimum χ^2 procedures. The low energy threshold was always less than 1 MeV and, for the 37 MeV measurement, a linear extrapolation of the measured energy spectra to zero yield at zero energy allowed the extraction of energy integrated cross section for the production of the various masses. This last procedure is supported by simple considerations on the value of the ratio P_{LAB}/P_{CM} in the Jacobian transforming CM to LAB cross section. Tables I and II collect the numerical values of the measured cross section while Fig. 5 presents a graph of the 40.3 MeV results showing a diffraction pattern interesting for the elucidation of the reaction mechanism.

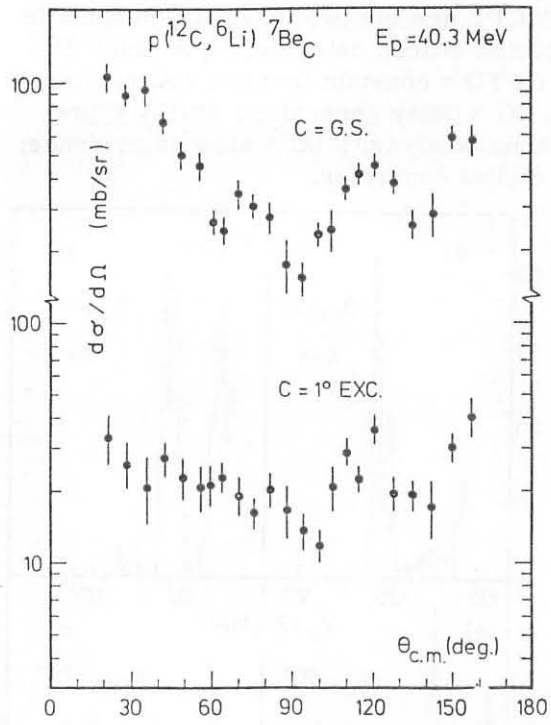

FIG. 5 - Differential cross sections of the direct reactions $^{12}C(p, ^6Li)^7Be$ proceeding to g. s. and 1° excited states in ^7Be, at E_p = 40.3 MeV.

The error shown in these Tables and graphs is an overall uncertainty taking into account statistics plus peak fitting procedures for the 40.3 MeV data and statistics plus extrapolation and angle integration procedures for the 37 MeV data. Some backward angle data at 40.3 MeV were obtained detecting recoiling ^7Be nuclei (in either the ground or first excited states) at forward angles. Angle aperture of the detectors has been always less than ± 1 degree and some measurements through the associated recoil have been averaged with the direct ^6Li measurements if the involved CM angles were within 2 degrees. In these cases an average angle has been indicated.

Further studies are in progress concerning the analysis of these reactions.

The technical support of Mr. P. Tempesta is gratefully acknowledged.

TABLE I - Measured values of the differential cross sections, at E_p = 40.3 MeV, for the reactions:

a) $^{12}C(p, {}^6Li)^7Be_{g.s.}$ b) $^{12}C(p, {}^6Li)^7Be_{0.431\,MeV}$

$\theta_{c.m.}$ (°)	$\frac{d\sigma}{d\Omega}$ (μb/sr)	$\theta_{c.m.}$ (°)	$\frac{d\sigma}{d\Omega}$ (μb/sr)
21.36	105.0 ± 15.2	21.46	33.2 ± 7.7
28.41	88.4 ± 10.2	28.54	25.8 ± 5.5
35.40	92.0 ± 14.1	35.58	21.8 ± 6.7
42.36	68.3 ± 7.1	42.55	27.2 ± 4.4
49.21	50.0 ± 6.5	49.43	22.6 ± 4.3
55.97	45.2 ± 6.3	56.21	20.7 ± 4.2
61.33	26.3 ± 3.3	59.55	20.9 ± 3.9
65.18	24.0 ± 3.1	63.85	22.6 ± 3.0
70.56	34.2 ± 4.8	70.07	19.0 ± 3.6
75.84	30.6 ± 3.3	75.76	16.1 ± 2.3
81.89	27.4 ± 3.8	81.83	20.1 ± 3.2
87.82	17.4 ± 4.3	88.18	16.6 ± 4.1
94.04	15.2 ± 2.6	94.02	13.6 ± 2.3
100.14	23.3 ± 2.7	100.14	11.8 ± 1.9
104.92	24.5 ± 4.8	105.32	20.7 ± 4.3
110.23	36.0 ± 3.9	110.63	28.6 ± 3.4
114.83	41.5 ± 3.9	114.87	22.3 ± 2.7
121.29	44.9 ± 4.7	120.99	35.4 ± 4.2
128.36	38.0 ± 4.3	128.11	19.3 ± 3.0
135.54	25.6 ± 3.3	135.32	19.1 ± 2.8
148.82	28.2 ± 5.8	142.63	17.1 ± 4.5
150.17	58.2 ± 6.1	150.03	30.4 ± 4.4
157.58	57.0 ± 8.4	157.46	40.7 ± 7.0

TABLE II - a) Differential cross section (mb/sr) at the shown angles and b) total cross section (mb) for the production of the indicated masses under 37 MeV proton bombardment of ^{12}C.

θ_{lab} / mass number	a) 50°	70°	90°	110°	b)
6	1.68 ± 0.24	0.69 ± 1.0	0.82 ± 0.12	0.30 ± 0.05	11.3 ± 1.5
7	1.80 ± 0.13	0.54 ± 0.05	0.28 ± 0.03	0.076 ± 0.01	12.1 ± 4.4
8	0.43 ± 0.11	0.22 ± 0.07	0.05 ± 0.01	0.042 ± 0.01	2.4 ± 0.5
9	0.34 ± 0.15	0.21 ± 0.07	0.62 ± 0.01	0.044 ± 0.01	2.0 ± 0.4
10	0.74 ± 0.26	0.18 ± 0.05	0.10 ± 0.02	0.056 ± 0.01	6.2 ± 3.4
11	12.6 ± 0.13	0.13 ± 0.01	0.58 ± 4x10^{-4}	0.41 ± 3.6x10^{-4}	54.8 ± 14

REFERENCES

(1) - C. Rolfs and H. P. Trauvetter, Ann. Rev. Nucl. Part. Sci. 28, 115 (1978), and references therein.

(2) - C. T. Roche, R. G. Clark, G. J. Mathews and V. E. Viola Jr., Phys. Rev. 14, 410 (1976), and references therein.

(3) - G. D'Erasmo, A. Pantaleo and V. Paticchio, A trasmission time detector for low energy light ions, to be published.